# Optimizing NB-IoT Communication Patterns for Permanently Connected mMTC Devices

Martin Stusek[1,2], Nikita Stepanov[3,4], Dmitri Moltchanov[2], Pavel Masek[1], Radek Mozny[1,2],
Andrey Turlikov[3], and Jiri Hosek[1]

[1]*Brno University of Technology, Faculty of Electrical Engineering and Communications, Dept. of Telecommunications,
Technicka 12, 61600 Brno, Czech Republic*
[2]*Tampere University, Unit of Electrical Engineering, Korkeakoulunkatu 7, 33720 Tampere, Finland*
[3] *St.-Petersburg State University of Aerospace Instrumentation, Bolshaya Morskaya 67, 190000 Saint-Petersburg, Russia*
[4] *Skolkovo Institute of Science and Technology, Bolshoy Boulevard 30, bld. 1, Moscow, Russia 121205*

*Abstract*—**The new types of industry-driven applications that need to be supported by low-power wide-area networks (LP-WANs), such as remote control or metering of devices within the massive machine-type infrastructures (e.g., Smart Grids), require a permanent connection to the remote server. In addition, there is also a shift in the communication paradigm, as the user equipment (UE) nodes are queried in regular and frequent intervals. Notably, the presence of this type of traffic may drastically deteriorate the performance of LPWAN technologies initially developed to support conventional use-cases characterized by non-synchronized transmissions. Though none of the LPWAN technologies is inherently designed to handle such demanding communication patterns, the narrowband Internet of things (NB-IoT) still stands for the best candidate as it operates within the license frequency spectrum. To optimize the delay performance of both types of traffic coexisting at the NB-IoT air interface, we propose an approach based on spreading the message transmission time instants of regular and stochastic traffic. We show an optimal value of the spreading interval minimizing the message transmission delay of regular traffic and propose a mathematical model to estimate its value. By parameterizing the model using a detailed measurements campaign of NB-IoT, we show that the optimal value of spreading interval and associated mean message delay is a linear function of the number of UEs. We report these values for a wide range of UEs in the coverage area of the NB-IoT base station and show that conventional stochastic traffic does not influence regular traffic performance.**

*Index Terms*—**Optimization, LPWAN, NB-IoT, Communication Patterns, Permanent Connectivity**

## I. INTRODUCTION

The transformational shift from communication networks designed to connect people towards industry-driven scenarios paved the way to massive machine-type communication (mMTC). The mMTC forces us to rethink how the deployed devices communicate through the network completely. We are witnessing the departure from the legacy communication use-cases proposed in the last decade for the Internet of things (IoT), following the irregular traffic defined by the International Telecommunication Union – Radiocommunication Sector (ITU-R) M.2412 requirements to the new applications characterized by the need for permanent network connectivity [1]. However, even for the low-power wide-area network (LPWAN) technologies, the performance can be compromised as they have been developed having sporadic irregular and unsynchronized communication in mind to serve both the regular and stochastic traffic [2].

The main goal of this paper is to asses the impact of this new type of traffic on the NB-IoT systems' performance [3]. To this aim, we first propose a simple approach of spreading the message transmission time instants of regular traffic in the presence of conventional stochastic transmissions. Further, we formulate a mathematical model of the NB-IoT cell, parameterize it with real measurements. Then, we analytically derive the mean message transmission delay for both traffic types as a function of system parameters. Finally, by utilizing both analytical and simulation approaches, we characterize the optimal value of the spreading interval and investigate system performance.

Our main contributions are as follows:
- the concept of spreading communication interval to improve delay performance of both regular and conventional stochastic traffic in NB-IoT deployments;
- mathematical model parameterized by measurement campaign of operational NB-IoT network to estimate the optimal value of the spreading interval and associated mean message transmission delay;
- NB-IoT network capacity planning based on the observations that the optimal value of the spreading interval and mean message delay of regular traffic linearly depends on the number of user equipment (UE)s.

The rest of the paper is organized as follows. In Section II we provide background on new applications emerging in IoT landscape. The system model is formulated, solved, and parameterized in Sections III - V. Numerical results are provided in Section VI, and conclusions are drawn in the last section.

## II. BACKGROUND AND RATIONALE

Aside from the well-known scenarios, such as environmental monitoring and asset tracking, smart electricity metering is being discussed the most now. Electricity distributors are seeking flexibility at every level of their business. As the communication network has to be reliable and resilient, utilities aim to get the most out of their investment, in the long run, to be prepared for whatever needs may arise in the future [4]. The

requirement for long-term operation of deployed smart grid meters or sensors is the one causing the most discussions these days. Trying to find communication technologies capable of creating and maintaining the advanced metering infrastructure (AMI), distributors are challenging the telco operators as their traditional partners [5], [6]. However, emerging types of applications are introducing novel requirements that were not part of the discussions before.

Focusing on the most critical one, let us discuss the communication logic that is now completely redesigned. The conventional approach, where each end device acts as the "source" and the central node performs in the role of "sink", no longer applies. Instead, in the next-generation communication networks, which are considered as the enablers for the smart grid scenarios, the transmission paradigm follows the "request-response" approach, which is by nature "client-originated". Notably, the capacity limitation of current cellular IoT technologies, i.e., NB-IoT and LTE Cat-M, represents the primary concern when switching from the legacy "source-sink" model. Therefore it will be crucial to consider this with today's supervisory control and data acquisition (SCADA) systems' architecture as it is expected that most of the data traffic in the industry networks will be transmitted via mobile networks.

Having all of the above-mentioned in mind, we focus on the coexistence of the regular and conventional stochastic traffic in the NB-IoT network, the preferred communication enabler for remote metering. In cooperation with the telecommunication operators and the electricity distributors, we build an analytical model capturing the random access procedure concerning the traffic patterns and network capacity planning.

## III. System Model

We first formulate a system model by capturing the relevant components of the considered system. Then, we proceed analyzing the system for performance measures of interest.

### A. Deployment

We consider a single NB-IoT cell with one resource block (RB) allocated for operation. The NB-IoT operation is assumed to be in guard-band or stand-alone mode within the licensed frequency spectrum. Furthermore, the network deployment is supposed to be well-provided by the telco operator, i.e., there are no other UEs in the cell with extremely weak channel conditions. For this reason, in what follows, we assume that the loss of packets due to incorrect reception is negligible. In such situations, the access phase becomes the dominant factor for performance degradation.

### B. Traffic Types

We consider two types of applications utilizing the resources of the NB-IoT system. The first, Type I UEs (regular), are those explicitly controlled from the remote application server, and thus they are always awake and keep their radio interface active. For this reason, during the whole operation lifetime, they are in a radio resource control (RRC) connected state,

as discussed later. The second, Type II UEs (stochastic), are conventional UEs going through the sleep-aware-transmit cycle. These UEs may represent periodic measurements, and their operational cycles are assumed to be asynchronous. We assume that the interarrival time between message transmission in this type of traffic is exponentially distributed with mean $\lambda_2^{-1}$.
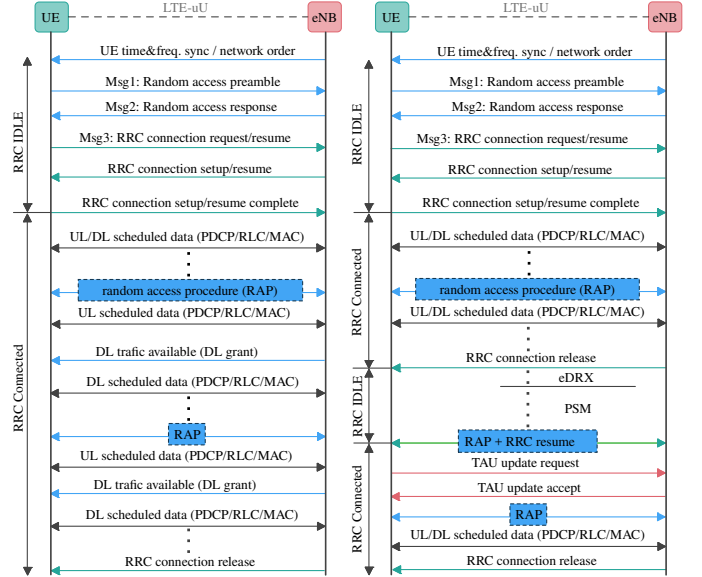


Fig. 1. NB-IoT access signalling: left – Type I UEs; right – Type II UEs.

*1) Random Access Phase in NB-IoT:* Following NB-IoT specification [7], see Fig. 1, UE is assumed to determine NB-IoT carrier by measuring the power of the received synchronization signals in the downlink (DL) direction and performing time and frequency synchronization together with Cell ID decoding. The time interval between synchronization information repetition may vary between 24 and 2604 ms [8]. Next, the narrowband physical broadcast channel (NPBCH) that carries the master information block (MIB) for 640 ms transmission time interval (TTI) is decoded. Also, overhead information about the cell characteristics is transmitted to the system information block type 1 (SIB1-NB) for 2560 ms and other SIB2-NB information from the base station (BS). More details can be found in [9].

Once synchronized, UE can configure the narrowband physical random access channel (NPRACH) resource and perform uplink (UL) transmission of preambles according to the network settings. So that both the number of repetitions and the transmit power are sufficient. The number of preamble repetitions can vary between 1 and 128. One preamble with the deterministic tone hopping pattern within a repetition unit consists of 4 groups of characters. Each group consists of 5 characters and a cyclic prefix ($66.67\,\mu s$ or $266.7\,\mu s$ for 10 or 40 km cell radius, respectively). For this reason, the random access attempt duration ranges between $5.6\,ms$–$819.2\,ms$ [10]. Upon reception on the BS side, it can correct the frequency and time offset and estimate timing advance (TA) for upcoming transmissions. NB-IoT specifies the minimum number of or-

thogonal preambles (sub-carriers) to be 12 out of 48 available. The data transfer phase is initiated in the narrowband physical downlink control channel (NPDCCH), which is utilized to transmit the downlink control information (DCI). Repetitions of this signal can range from 1 up to 2048 times [11].

The above-mentioned access phase is performed differently for two considered types of traffic. An example could be the initial access with transmission from RRC idle to RRC connected state, followed by message transmission. Here, the random access would be used for both the access phase and following message transmission, with subsequent RRC release. For example, if UE wants to transmit the data from RRC idle, it would first perform an RRC resume procedure requiring random access. After that, the device asks for UL/DL grants, and the message is transmitted [11].

*2) Modeling Assumptions:* We consider a slotted system, with time divided into slots. The slot duration is 10 ms, which equals the duration of one LTE frame and specifies the minimum random access time without repetitions. There is a fixed number of Type I UEs in cell coverage, $N_1$. The applications query these UEs at the beginning of the regular time interval of duration $T$. This time interval depends on the application type and can be on a timescale of minutes to hours. Notably, parameters $D_1$ and $D_2$ represent the delay samples in this case. Upon request, all $N_1$ UEs attempt message transmission by performing the NB-IoT random access procedure. To alleviate this issue, we consider a mechanism where UEs may delay transmission by some time uniformly distributed over $(T, T + \tau_1)$, see Fig. 2.
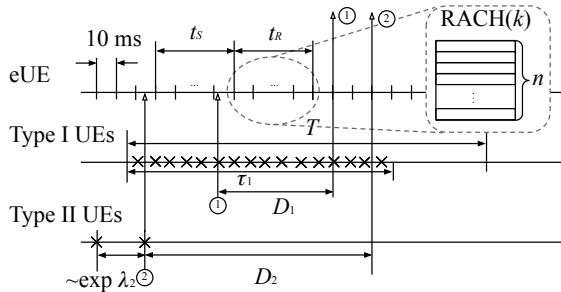


Fig. 2. Timing diagram of the system operation.

The rationale behind the procedure is as follows. When $\tau_1$ is small, the load on the system is high, and both Type I and Type II UEs experience large delays due to RACH conflict resolution. When $\tau_1$ increases, the initial Type I UEs RACH requests become more evenly distributed, reducing the delay. However, when $\tau_1$ is too large, the mean delay of Type I UEs again increases due to delayed initial RACH access attempts. Furthermore, the choice of the spreading interval $\tau_1$ also affects mean delays of Type II UEs as both types of devices have a mutual influence on latency. In practice, the interval $\tau_1$ can be configured at the application server. Alternatively, UEs can be instructed to initialize their first access attempt randomly and uniformly over $(T, T + \tau_1)$.

Upon generating a message, both UE types initiate the random access procedure in the next time slot. We assume

that the probability of starting the random access procedure is $p = \min(n/k, 1)$, where $n$ is the number of preambles, $k$ is the UEs that compete in a slot. As shown in [12], [13] this approach minimizes the delay of UEs.

*3) Metrics:* We are interested in answering two questions: (i) what is the mean delay of Type I and Type II traffic, $E[D_1]$ and $E[D_2]$, respectively, and (ii) what is the optimal choice of $\tau_1$ minimizing message transmission delay of Type I UEs.

## IV. SYSTEM ANALYSIS

We observe the system at discrete times with a slot duration of $t_R$. Time slot 0 corresponds to the beginning of the query interval of Type I UEs. Let us denote by $N_t$ the number of active UEs of both types with a message ready for transmission and have not yet received access. Recalling the assumptions introduced in Subsection III-B2, the number of active UEs in the time interval $t + 1$ is related to the number of active UEs in the time interval $t$ as

$$N_{t+1} = \begin{cases} N_t - T(N_t) + V_t^1(N_t) + V_t^2 & t \cdot t_R \leq \tau_1 \\ N_t - T(N_t) + V_t^2 & t \cdot t_R > \tau_1 \end{cases}, \quad (1)$$

where $T(N_t)$ is the number of successful transmissions when the system has $N^t$ active UEs, $V_t^1(N_t)$ and $V_t^2$ are the numbers of Type I and Type II UEs, respectively, that become active in the slot $t$, provided that $N_t$ is the number of active UEs at the beginning of the slot $t$.

The trajectory of this stochastic process obtained using computer simulations is illustrated in Fig. 3. We specifically note that this process is not Markov in nature, complicating its accurate characterization. In order to capture the basic characteristics of this process, in what follows, we resort to the approximation techniques. Particularly, instead of considering the stochastic evolution of $\{N_t, t = 0, 1, \dots\}$ explicitly according to (1), we introduce and investigate properties of an associated deterministic process characterizing the fluid approximation of the number of active UEs, $\overline{N_t}$, over time.

Since active UEs are assumed to transmit in a slot with probability $p = \min(n/k, 1)$, see Subsection III-B2, we have

$$E[T(N_t)] \approx ne^{-1}. \quad (2)$$

Furthermore, by recalling that Type I UEs are instructed to choose the transmission slot uniformly over the interval from 1 to $\tau_1$, we can write for $V_t^1(N_t)$
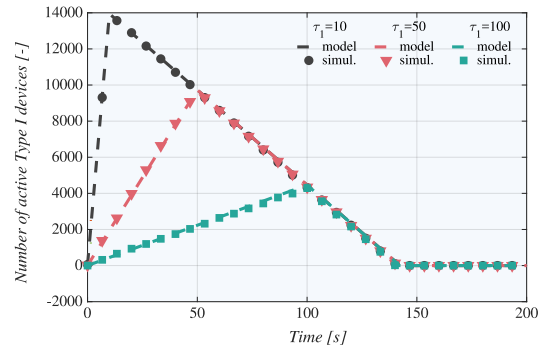


Fig. 3. Number of active UEs of the Type I.

$$E[V_t^1(N_t)] = m_1 t_R / \tau_1. \tag{3}$$

Finally, note that the arrival intensity of Type II UEs remains constant over time implying that

$$E[V_t^2] = \lambda_2 t_R. \tag{4}$$

By utilizing the results (2)–(4) we can apply the fluid approximation, see [14], and write the recurrent relation for $\overline{N_{t+1}}$ approximating the evolution of the mean value of the stochastic process $\{N_t, t = 0, 1, \dots\}$ defined as follows

$$\overline{N_{t+1}} = \begin{cases} \overline{N_t} - ne^{-1} + \frac{m_1 t_R}{\tau_1} + \lambda_2 t_R & t \cdot t_R \le \tau_1 \\ \overline{N_t} - ne^{-1} + \lambda_2 t_R & t \cdot t_R > \tau_1 \end{cases}. \tag{5}$$

The evolution of the original stochastic process of the number of active UEs $\{N_t, t = 0, 1, \dots\}$ and the associated deterministic mean process are both shown in Fig. 3 for the case of $ne^{-1} < m_1 t_R / \tau_1$ and multiple values of the spreading time $\tau_1$. As one may observe, process $\{\overline{N_t}, t > 0\}$ closely approximates the original one implying that the former can be utilized to accurately approximate the mean delay of message transmission delay for both Type I and Type II UE devices. We now proceed deriving $E[D_1]$ and $E[D_2]$.

Let us denote by $T'$ the time instant when all the Type I UEs leave the system after successful service. Consider also $d$, defined as the mean message transmission delay. These metrics are related to each other as follows

$$d = \left( \sum_{t=1}^{T'} \overline{N_t} \right) \Big/ (m_1 + \lambda_2 T'), \tag{6}$$

where the numerator is the only unknown.

Consider the term $\sum_{t=1}^{T'} E[N_t]$. Observing the structure of $\{\overline{N_t}, t > 0\}$ in Fig. 3, one may deduce that the sought sum coincides with the area of a triangle with a base $(0, T')$ in Fig. 3. The height of the triangle corresponds to the maximum level of $E[N_t]$ coinciding with the following value

$$m_1 - ne^{-1} \tau_1 / t_R + \lambda_2 \tau_1. \tag{7}$$

The base of the triangle is exactly $T'$. This length can be written as $T' = \tau_1 + X$, where $X$ is determined by

$$X = \frac{m_1 - ne^{-1} \frac{\tau_1}{t_R} + \lambda_2 \tau_1}{ne^{-1}} = \frac{m_1}{ne^{-1}} - \frac{\tau_1}{t_R} + \frac{\lambda_2 \tau_1}{ne^{-1}}. \tag{8}$$

Solving (8) with respect to $T'$, we get

$$T' = \frac{\tau_1}{t_R} + X = \frac{m_1}{ne^{-1}} + \frac{\lambda_2 \tau_1}{ne^{-1}}. \tag{9}$$

Now, the area of the triangle is determined by

$$\sum_{t=1}^{T'} E[N_t] = \left( m_1 - ne^{-1} \frac{\tau_1}{t_R} + \lambda_2 \tau_1 \right) \times$$
$$\times \frac{1}{2} \left( \frac{m_1}{ne^{-1}} + \frac{\lambda_2 \tau_1}{ne^{-1}} \right). \tag{10}$$

Substituting (10) into (6) we obtain

$$d = \frac{1}{2ne^{-1}} \left( m_1 - ne^{-1} \frac{\tau_1}{t_R} + \lambda_2 \tau_1 \right). \tag{11}$$

Once $d$ is determined, we are in a position to calculate the mean transmission delays of Type I and Type II UEs $E[D_1]$ and $E[D_2]$, by summing up delay components as

$$E[D_1] = \tau_1 / 2 + d,$$
$$E[D_2] = T'(d + t_S) + (T - T')(t_S + t_R)/T. \tag{12}$$

Substituting (11) into (12) and differentiating between two cases, $t \cdot t_R \le \tau_1$ and $t \cdot t_R > \tau_1$ in (5), we get the final result for Type I UE mean message transmission delay in the following form

$$E[D_1] = \begin{cases} \frac{1}{2} \left( \frac{m_1}{ne^{-1}} + \frac{\lambda_2 \tau_1}{ne^{-1}} \right) & ne^{-1} < \frac{m_1 t_R}{\tau_1} + \lambda_2 \\ \frac{1}{2} \tau_1 & ne^{-1} > \frac{m_1 t_R}{\tau_1} + \lambda_2 \end{cases}. \tag{13}$$

To provide the final expression for mean message transmission delay of Type II UEs we follow the same approach by substituting (11) into (12). Note that the mean delay is negligible when $ne^{-1} < m_1 t_R / \tau_1$. We thus obtain

$$E[D_2] = \frac{T'(d + t_S) + (T - T')(t_S + t_R)}{T}, \tag{14}$$

for $ne^{-1} < m_1 t_R / \tau_1 + \lambda_2$ and $E[D_2] = 0$ otherwise.

## V. PARAMETERIZATION CAMPAIGN

The development of the proposed models relies on several timing assumptions of the NB-IoT technology. However, these assumptions heavily depend on the actual implementation of NB-IoT release (defined by 3GPP), mobile network configuration (operator specific), UE design, e.g., number and selection of subcarriers for random access, number of repetitions for all communication duties, and number of utilized subcarriers for transmission. All mentioned parameters influence the time required for synchronization, RRC state transmissions, and message transmissions.

To get the representative results, which we can utilize as inputs of actual NB-IoT implementation to our models, we carried out a measurement campaign for Type I and Type II UEs on mobile networks to parameterize the system. However, it is important to mention that the measurement campaign intended to get parameters of non-interfered devices within a network with specific parameter settings. The measurement setup described below is depicted in Fig. 4. As for the mobile network, we utilized the current 3rd generation partnership project (3GPP) Release 13 implementation of NB-IoT from one of the mobile operators in the Czech Republic.

From the UE perspective, as the representatives of both device types, we utilized boards fitted with BC68 NB-IoT modules from the company Quectel. The Type I device represented on-demand reading of DLMS protocol values used by electricity meters. To mimic the DLMS behavior, the Type I device was set to transmit 200 B payload in 15 minutes intervals as a request to remote DLMS server with transmission control protocol (TCP) on transport layer to which server responded with the same amount of 200 B. Similarly, as the traditional sensor representative, the Type II device transmitted 200 B messages to a remote server in 1-hour intervals over user datagram protocol (UDP) on the transport layer. The device
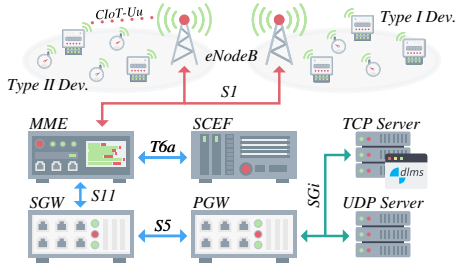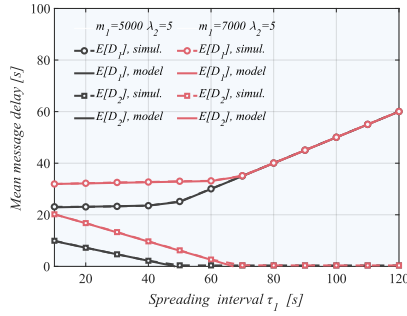
Fig. 4.  Measurement campaign setup.



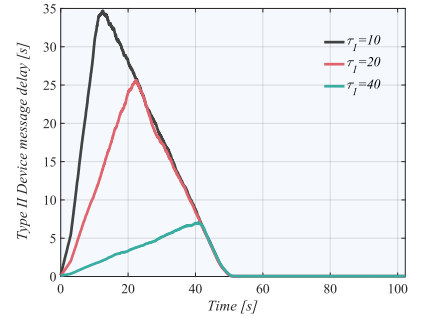Fig. 5.  Mean message delay for different $m_1$.



Fig. 6.  Smoothed message delay.

spent the rest of the 1-hour interval in power saving mode (PSM). After waking up from PSM, the RRC connection and tracking area update (TAU) needed to be performed before the subsequent message transmission.

We monitored the UE behavior from its debug serial port to get detailed timing assumptions for a model. The radio interface activity was measured using the radio spectrum analyzer Blade RF 2.0 software-defined radio (SDR) for 24 h long measurement. As the devices were placed near an indoor cell, we achieved excellent and stable radio conditions with reference signal received power (RSRP) between $-60$ to $-65$ dBm. Furthermore, spectrum analysis confirmed that other devices induced no interference.

Based on the measurements, we obtained analytical model parameters, summarized in Table I. All the assumptions are based on average values from the results and were measured as follows: (1) time to synchronization was set as the time for the initial time, and frequency synchronization together with gathering information about surrounding cells, (2) the random access preambles were set with two repetitions and selection from 12 subcarriers, (3) the collision-free RAP was set as the RAP phase up to the Msg3, (4) the 200 B message transmission time was determined as radio transmissions without RAP, TAU, and RRC connection phases, (5) the message handling time was set as the time for UE to process messages.

## VI. NUMERICAL RESULTS

In this part, empowered with the parameters extracted from the measurement campaign, we assess the delay performance of Type I and Type II UEs and identify the optimal value of the spreading interval $\tau_1$ minimizing the delay of Type I UE messages. We first start with comparing our model results with the computer simulations and then investigate the effect of system parameters on the optimal value of $\tau_1$.

Fig. 5 shows the comparison between the model and simulation data. The latter have been obtained by custom-designed discrete event simulation (DES) framework by explicitly modeling the message transmission process of Type I and Type II UEs according to NB-IoT access and data transmission procedures. The parameters have been aligned with those obtained during the measurement campaign in Section V. To capture possible dependence between successive query intervals that may lead to the deviation between model and computer simulations, we averaged the simulation results over

TABLE I
INPUT PARAMETERS FOR ANALYTICAL MODEL.

| Parameter name | Symbol | Value |
|---|---|---|
| Number of preambles | $n$ | 12 |
| The time to synchronization | $t_S$ | 30 slots |
| Temporary collision-free RAP | $t_R$ | 4 slots |
| Message handling time | $t_H$ | 1 slot |
| Data transfer time | $t_{data}$ | 35 slots |
| Message period for I Type | $T$ | 1 - 60 min |
| Number of user equipment of I Type | $m_1$ | 100-10000 |
| Input flow rate of II Type | $\lambda_2$ | 1-100 per sec |

100 query intervals. Further, we note that following ITU-R M.2412, we have assumed that Type II UEs generate messages every 2 hours, implying that the considered value of $\lambda_2 = 5$ msg/s corresponds to 3600 Type II UEs.

By comparing the results presented in Fig. 5, one may observe that the model is capable of correctly predicting the full mean message transmission delay of Type I UEs. However, at first glance, the proposed approach does not allow to improve this metric as the delay stays flat and then increases. The rationale is that the gain of spreading Type I message sending requests over $\tau_1$ is compensated by the increased delay of the first transmission attempts of UE. The second interesting observation is that the Type II UE delay is relatively small compared to Type I UE delays.

We clarify the statements mentioned above by analyzing the instantaneous delay of Type II messages shown in Fig. 6. To provide a clear visual illustration of the trends in data, we applied a moving average filter. As one may observe, Type I UEs heavily impact the delay of Type II messages over the spreading interval $\tau_1$. Once it ends, the delay gradually decreases and then reaches small values typical for the system with only Type II UE load. Secondly, observe that this trend is also characteristic of the actual delay of Type I UEs during the spreading interval $\tau_1$ (excluding the term $\tau_1/2$).

Thus, the increase in the value of $\tau_1$ allows to decrease the instantaneous delay of both Type I and Type II UEs. The developed analytical model provides a simple way to determine the optimal spreading time $\tau_1$ minimizing the delay of both types of UEs by estimating the point where the slope of the mean delay function changes.

Having evaluated the developed model's capabilities, we are in a position to consider the effect of the number of UEs on the mean message delay for different values of $\tau_1$ illustrated
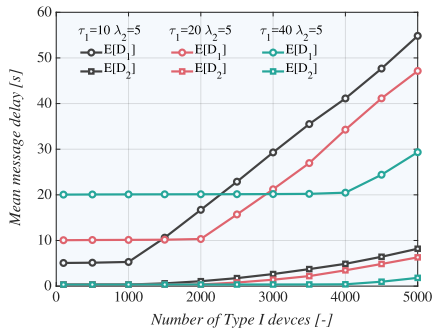
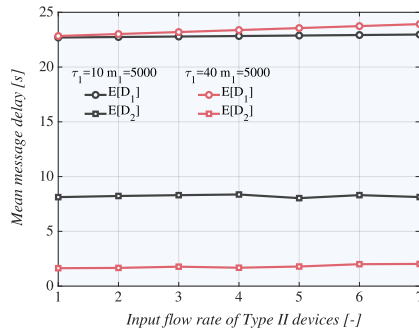Fig. 7.  Delay as a function of Type I devices.



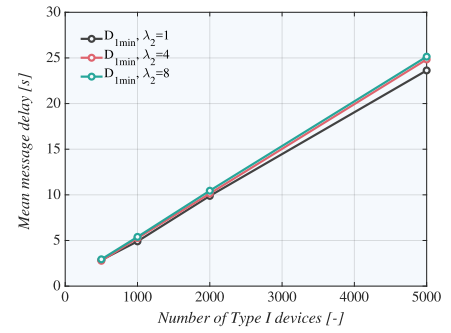Fig. 8.  Delay as a function of Type II devices.



Fig. 9.  Type I device optimal message delay.

TABLE II
OPTIMAL VALUES OF SPREADING INTERVAL $\tau_1$.

| Type I UEs [-] | 500 | 1000 | 2000 | 5000 |
|---|---|---|---|---|
| Optimal $\tau_1$ [s] | 5 | 10 | 20 | 45 |
| Mean $D_1$ [s] | 2.5 | 5 | 10 | 23.7 |

in Figs. 7 and 8. First of all, in Fig. 7 we observe that the number of Type I UEs only slightly affects the mean delay of Type II UEs resulting in an insignificant increase. Similar conclusions can be made for $\tau_1$. The rationale is that $\tau_1$ is much smaller than the considered query interval $T$, which is set to 15 minutes in our simulations. However, for a given value of $\tau_1$, the number of Type I UEs heavily affects the mean delay of Type II UEs. At the same time, we observe in Fig. 8 that Type II traffic does not produce any substantial effect on Type I UE delay performance.

Finally, we show the mean Type I UE message delay for different values of Type I UEs and intensity of Type II traffic corresponding to the optimal values of spreading interval $\tau_1$ in Fig. 9. As one may observe, the sought metric scales linearly with the number of Type I UEs, and its slope is almost independent of Type II traffic intensity $\lambda_2$. These two properties simplify estimating the value of mean Type I UE delay corresponding to the optimal spreading interval for different traffic conditions. The associated optimal spreading intervals and delays are demonstrated in Table II. As one may observe, $\tau_1$ also increases linearly.

## VII. CONCLUSIONS

In this paper, we addressed the problem of the coexistence of regular and stochastic traffic in NB-IoT systems. To this aim, we built an analytical model capturing the essentials of the random access procedure of two considered traffic types over an application query interval and parameterized it using real measurements. Furthermore, to optimize the mean delay performance of regular traffic, we introduced the notion of spreading interval and utilized the development model to assess its optimal values leading to the minimal regular traffic delay.

Our results show that the number of UEs generating regular traffic heavily affects the mean delay of both traffic types. On the other hand, practical values of conventional sporadic traffic do not provide any noticeable impact on regular traffic. Finally, the spreading interval's optimal values minimize the

delay of regular traffic. The optimal values of this interval and the associated optimal delay of the regular traffic type linearly depend on the number of UEs generating regular traffic. The approach proposed in this work allows determining the maximum number of Type I UEs supported at NB-IoT BS with given delay guarantees.

## REFERENCES

[1] M. Series, "Guidelines for Evaluation of Radio Interface Technologies for IMT-2020," 2017.
[2] A. K. Sultania, F. Mahfoudhi, and J. Famaey, "Real-Time Demand Response Using NB-IoT," *IEEE Internet of Things Journal*, vol. 7, no. 12, pp. 11863–11872, 2020.
[3] M. S. Bali, K. Gupta, K. K. Bali, and P. K. Singh, "Towards Energy Efficient NB-IoT: A Survey on Evaluating its Suitability for Smart Applications," *Materials Today: Proceedings*, 2021.
[4] A. Antonowicz, P. Derbis, M. Nowak, and A. Urbaniak, "Smart Meter in Voltage Control System of Power Network," in *2020 21th International Carpathian Control Conference (ICCC)*, pp. 1–6, 2020.
[5] P. Masek, M. Stusek, K. Zeman, J. Hosek, K. Mikhaylov, S. Andreev, Y. Koucheryavy, O. Zeman, J. Votapek, and M. Roubicek, "Tailoring NB-IoT for Mass Market Applications: A Mobile Operator's Perspective," in *2018 IEEE Globecom Workshops (GC Wkshps)*, pp. 1–7, 2018.
[6] S. R. Ullah Kakakhel, A. Kondoro, T. Westerlund, I. Ben Dhaou, and J. Plosila, "Enhancing Smart Grids via Advanced Metering Infrastructure and Fog Computing Fusion," in *2020 IEEE 6th World Forum on Internet of Things (WF-IoT)*, pp. 1–6, 2020.
[7] 3GPP, "LTE; Evolved Universal Terrestrial Radio Access (E-UTRA);LTE physical layer;" TS 36.201 V14.1.0, ETSI, Apr. 2017.
[8] A. Adhikary, X. Lin, and Y.-P. E. Wang, "Performance Evaluation of NB-IoT Coverage," in *2016 IEEE 84th Vehicular Technology Conference (VTC-Fall)*, pp. 1–5, IEEE, 2016.
[9] O. Liberg, M. Sundberg, E. Wang, J. Bergman, and J. Sachs, *Cellular Internet of Things: Technologies, Standards, and Performance*. Academic Press, 2017.
[10] L. Feltrin, G. Tsoukaneri, M. Condoluci, C. Buratti, T. Mahmoodi, M. Dohler, and R. Verdone, "Narrowband IoT: A Survey on Downlink and Uplink Perspectives," *IEEE Wireless Communications*, vol. 26, no. 1, pp. 78–86, 2019.
[11] M. Kanj, V. Savaux, and M. Le Guen, "A Tutorial on NB-IoT Physical Layer Design," *IEEE Communications Surveys & Tutorials*, 2020.
[12] M. Koseoglu, "Lower Bounds on the LTE-A Average Random Access Delay Under Massive M2M Arrivals," *IEEE Transactions on Communications*, vol. 64, no. 5, pp. 2104–2115, 2016.
[13] O. Galinina, A. Turlikov, S. Andreev, and Y. Koucheryavy, "Stabilizing Multi-channel Slotted Aloha for Machine-type Communications," in *2013 IEEE International Symposium on Information Theory*, pp. 2119–2123, IEEE, 2013.
[14] L. Kleinrock, "Theory," *Queueing systems*, vol. 2, 1975.